HHS Public Access

Author manuscript

Mol Psychiatry. Author manuscript; available in PMC 2016 February 01.

Published in final edited form as:

Mol Psychiatry. 2015 August ; 20(8): 974–985. doi:10.1038/mp.2014.106.

Gsx1 Expression Defines Neurons Required for Prepulse Inhibition

Sadie A. Bergeron, Ph.D.[1], **Nicole Carrier, Ph.D.**[1,2], **Grace H. Li, B.Sc.**[1], **Sohyun Ahn, Ph.D.**[1], and **Harold A. Burgess, Ph.D.**[1,*]

[1]Program in Genomics of Differentiation, Eunice Kennedy Shriver National Institute of Child Health and Human Development, Bethesda, MD 20892, USA

Abstract

In schizophrenia, cognitive overload is thought to reflect an inability to suppress non-salient information, a process which is studied using prepulse inhibition of the startle response. Prepulse inhibition is reduced in schizophrenia and routinely tested in animal models and pre-clinical trials of antipsychotic drugs. However the underlying neuronal circuitry is not well understood. We used a novel genetic screen in larval zebrafish to reveal the molecular identity of neurons that are required for prepulse inhibition in fish and mice. Ablation or optogenetic silencing of neurons with developmental expression of the transcription factor Gsx1 produced profound defects in prepulse inhibition in zebrafish, and prepulse inhibition was similarly impaired in Gsx1 knockout mice. Gsx1 expressing neurons reside in the dorsal brainstem and form synapses closely apposed to neurons which initiate the startle response. Surprisingly brainstem Gsx1 neurons are primarily glutamatergic despite their role in a functionally inhibitory pathway. As Gsx1 plays an important role in regulating interneuron development in the forebrain, these findings reveal a molecular link between control of interneuron specification and circuits which gate sensory information across brain regions.

Keywords

prepulse inhibition; startle; Gsx1; interneuron; glutamatic acid; zebrafish

Introduction

Schizophrenia is a severe neurological disorder whose etiology includes an important but poorly understood neurodevelopmental component [1]. A direct consequence of abnormal neural development may be cognitive impairments, which are observed in young children well before the onset of psychosis [2–3]. Cognitive deficits result in part from non-salient thoughts and sensory information flooding the mind with irrelevant percepts due to impaired

*6 Center Drive, Building 6B, Rm 3B308, Bethesda, MD 20892, burgessha@mail.nih.gov, tel: 301-402-6018; fax: 301-496-0243.
[2]Current address: University of Texas Health Science Center, Department of Pharmacology, San Antonio, TX 78229, USA

Conflict of interest

The authors declare no conflict of interest.

central filtering mechanisms [4–6]. Neuronal filtering mechanisms are studied using prepulse inhibition of the startle reflex (PPI), a paradigm in which a weak 'prepulse' occurring 10–500 ms before a sudden intense stimulus suppresses the startle response [7–8]. Because disrupted PPI is observed in individuals at high risk for developing psychosis, abnormalities may reflect disturbances in neural development that predispose these individuals to disease [9].

Genetic analyses of large patient cohorts are now yielding many candidate genes which contribute to schizophrenia risk making new tools for investigating the causal role of these genes essential [10]. Animal models with a well defined neuronal substrate for disease-relevant behaviors are an invaluable asset for investigating how genetic or environmental disturbances lead to neurological impairment. Supporting the use of PPI as an endophenotype which can be investigated using animal models, PPI defects in schizophrenia are present in prodromal phases of the disease and in unaffected relatives [11–12]. Measurements of PPI in animal models are a standard method for analyzing the effects of genetic and pharmacological manipulations. However neuronal circuitry which mediates PPI is not fully understood, limiting the insights that these models can offer. Defining the precise identity and pattern of synaptic connectivity of neurons required for PPI would thus illuminate a substrate for investigating the effects of gene mutations which increase risk for schizophrenia and promote rational design of therapeutic interventions [13].

Systems neuroscience approaches have shown that core circuitry for PPI resides in the brainstem and that partially overlapping mechanisms mediate PPI at different interstimulus intervals (ISIs) between the prepulse and the startling stimulus [14–16]. However detailed analysis of neuronal mechanisms for PPI in mammals remains a formidable challenge [17]. In contrast startle circuitry in fish is relatively simple and is therefore an attractive system in which to dissect neuronal connectivity. Acoustic/vibrational stimuli elicit rapid escape responses triggered by the Mauthner cells, a single bilateral pair of giant reticulospinal neurons which are similar in position and function to the central brainstem neurons for the mammalian acoustic startle response (ASR) [18–19]. Because Mauthner-driven startle responses are all-or-nothing events, PPI is manifest as a reduction in the probability of eliciting a startle response, rather than a reduction in the magnitude of the response as in mammals [20, 21]. PPI is robustly induced in larval zebrafish and reproduces salient features of the response in mammals, including the effective ISI and susceptibility to drugs that alter dopaminergic and glutamatergic neurotransmission [20, 22]. However the identity of neurons which inhibit the startle response during PPI remains unknown. Here we exploited the amenability to genetic screens and less complex brain structure of larval zebrafish to reveal the molecular identity of neurons required for PPI in this species. We then extended our work to behavioral analysis of a mouse model to confirm that our findings are pertinent to mammals.

Methods

Zebrafish husbandry

Construction of the transgene used to recover enhancer trap line *Et(REx2-SCP1:Gal4ff)y252* has been reported [23] but briefly, this transgene contains the reduced toxicity Gal4 variant

Gal4ff [24] driven by a minimal promoter consisting of tandem NRSE elements (REx2) and the supercore promoter 1 (SCP1) [25]. The *UAS:Kaede* transgenic line is *Tg(UAS:Kaede)s1999t* [26]. *J1229* is *Gt(T2KSAG)j1229a* [27]. *4xUAS:GFP is Tg(4xUASnr:GFP)c369* [28]. *vGlut:DsRed* is *TgBAC(vglut2.1:DsRed)* and *glyt2:GFP* is *TgBAC(glyt2:GFP)* [29]. *Tg(UAS:nfsB-mCherry)* fish were generated as previously reported [26]. The UAS:Arch3 transgenic line was generated from a 14xUAS-E1b:Arch3-TS-CFP-ER transgene which was constructed as follows. Zebrafish codon optimized cerulean (Genscript) was amplified by PCR, adding the Kir2.1 membrane trafficking signal (TS) at the N-terminal and an endoplasmic reticulum (ER) export signal at the C-terminal as described for eNpHR3.0 [30], then cloned into pT1UMP [31]. SS-PRL-Archaerhodopsin-3 [32] was synthesized, codon optimized for zebrafish (Genscript) then amplified by PCR and cloned in frame with the TS-CFP-ER cassette. The plasmid was injected into one cell stage embryos with Tol1 transposase [33] and founders screened to isolate transgenic line *Tg(UAS-E1b:Arch3-TS-CFP-ER)y259*. The *UAS:lynTagRFPT* line is *Tg(UAS-E1b:BGi-lynTagRFPT)y260* which was made using Tol1 transgenesis using a previously described plasmid [31]. For the *UAS:Synaptophysin-RFP* line overlapping extension PCR was used to fuse synaptophysin, amplified from UAS:Synaptophysin-EGFP [34] and zebrafish optimized TagRFPT. The product was cloned into pT1UMP and injected as above to isolate line *Tg(UAS-E1b:Synaptophysin-TagRFPT)y261*. For the *UAS:nls-GFP* line zebrafish codon optimized emerald GFP was synthesized (Genscript), PCR amplified adding the SV40 large T antigen nuclear localization sequence (MAPKKKWKV) to the N-terminal, cloned into pT1UMP and injected to isolate line *Tg(UAS-E1b:BGi-NLS-emGFP)y262*. All lines were maintained on a Tubingen long fin background and embryos raised in E3 medium supplemented with 1.5 mM HEPES pH 7.3 (E3/h) at 28°C on a 14:10 light:dark cycle. Additional details of plasmid construction are available on request. All zebrafish protocols were approved by the NICHD animal care and use committee.

Mice

Gsx1 knockout mouse heterozygotes [35](kind gift of K. Campbell) were maintained on a CD1 background as in previous generations. Heterozygous mice were incrossed to non-littermates to generate litters of $Gsx1^{+/+}$, $Gsx1^{+/-}$, $Gsx1^{-/-}$ siblings for behavioral testing. Using the AIMS neonate ID system, sibling mice were genotyped at postnatal day (P)7–10 by PCR analysis of tail DNA extracted using the DirectPCR Tail buffer system and the manufacturer's protocol (Viagen). Genotyping primers were: CGGGTGAAGCACAAGAAAGAAG; CCAATGGTCCTCTAAAAGGCG; GGTTCATCATCACTAATCACGACG; CGCTGTTCTCCCTCTTCCTCATCTC resulting in a 220 bp band for the wild type allele and a 150 bp band for the knockout allele. Litters were maintained at no more than 8 pups per dam to promote mutant survival and to match group size as an additional control. All experimental protocols were approved by the NICHD animal care and use committee.

Transgene mapping

Linker mediated PCR [36] was used to map the insertion site in *y252*. The site was confirmed by PCR on single embryos using chromosome 5 specific primer 5-TGCTTGTTGCTTGTTTTTGC with primer 5-TTGAGTAGCGTGTACTGGCATT,

specific to one of the Tol2 arms yielding a 347 bp band for the transgene locus. A single band was present in all *Kaede* positive embryos from a *y252; UAS:Kaede* outcross to TL (N = 31). For subsequent genotyping of *y252*, a multiplex PCR strategy was used, with primers 5-AGCAGAAATGTGCATCAAC and 5-TTGCTTGTTTTTGCAGTTGG which produce a 328 bp band for the wildtype genomic locus and a third primer 5-CAAGAATCTCTAGTTTTCTTTCTTGCT, yielding a 221 bp band for the transgene locus.

Zebrafish behavior

For screening Gal4 lines, each line was crossed to a *UAS:nfsB-mCherry* transgenic line allowing cell specific and temporally controlled ablation using metronidazole treatment [37–38]. Sibling larvae were sorted into strongly-expressing mCherry and non-expressing groups and both groups were treated from 3–5 dpf with 10 mM metronidazole in E3/h medium for ablation of nitroreductase-mCherry expressing neurons. Ablation was confirmed visually by checking for loss of patterned mCherry expression. Behavioral testing was performed after 24 h recovery from the treatment, at 6 dpf. Zebrafish larvae show two forms of startle response distinguished by latency and kinematics, Mauthner cell mediated short-latency c-start (SLC) and non-Mauthner long-latency c-start (LLC) responses [20, 39]. SLC responses are susceptible to PPI [20] and were therefore the focus of this study. In the initial PPI screen, a 500 ms ISI was used. For Arch3 experiments larvae were embedded in 2 % low melt agarose in a glass bottom Petri dish before the area caudal to the fins was removed so that the tail was free. The dish was mounted in a custom stage printed in ABS plastic using a uPrint rapid prototyping system (Stratasys, Eden Prairie, MN) attached to a compound microscope (Axioimager.A1, Zeiss). Tail movements were imaged with a camera (μEye IDS-1545LE-M, 1stVision, Andover, MA) and objective (infiniGage CW with 0.50x mag precision spacer) mounted in place of the condenser. To determine the latency threshold for distinguishing short-latency startle responses in head fixed embryos, larvae were tested 20 times with a vibrational stimulus and responses recorded at 200 Hz. Images were scored manually to determine the earliest time of tail movement. A 10X objective was used to focus light pulses (520 nm) delivered by a high power LED (UHP-Mic-LED-520, Prizmatix, Israel) onto the head of the larva. Infra-red illumination was used to visualize the tail, with light used for the Arch3 stimulus excluded with a long pass filter in the camera objective (NT54-662, Edmunds). Stimulus timing and image acquisition was coordinated using a digital-analog card (PCI-6221, National Instruments, Austin, TX) controlled by DAQtimer event control software [20]. 520 nm illumination was started 500 ms prior to the stimulus to inhibit *y252* neurons. To exclude trials in which larvae were engaged in spontaneous locomotor activity during presentation of the startle stimulus, images were collected 32 and 16 ms before the startle stimulus to check for tail movements. An image was taken 20 ms after the startle stimulus to identify short latency startle responses and another image 80 ms after the pulse to identify long latency startle responses. For PPI trials, the pulse was delivered 500 ms after the prepulse. LED illumination was present over the course of the entire trial when used (642 ms for startle, 1110 ms for PPI). Inter-trial intervals were 20 s long, and conditions were presented in a pseudorandom order across the experiment. Control trials included LED alone trials and no stimulus trials. Startle response, PPI experiments, baseline spontaneous movement, dark flash responses, kinematic analysis of swimming and the visual motor response were measured as previously described [20, 40, 41].

For the MK801 experiment, 6 dpf larvae were treated in groups of 20 per 6 cm dish with 30 μM MK801 (M107, Sigma) in 1% DMSO for 20 minutes before behavioral testing. Controls received 1% DMSO only.

Mouse behavior

Acoustic startle and PPI were measured using the SR-Lab Startle Response System (San Diego Instruments, San Diego, CA). P20–21 pups were transported in a standard plastic cage with the dam and littermates to a lit holding room just outside of the testing room where they adapted for 30 minutes prior to testing. Two mice were removed at a time from their home cage for analysis, one per available testing chamber. Mice were enclosed so that they could just turn around inside Plexiglas tubes within the lit and ventilated testing chambers and allowed to acclimate for 3 minutes prior to the session. Background noise level was maintained at 65 dB for the duration of the test including during acclimation. For acoustic startle testing, mice were presented with 60 trials using a variable inter trial interval of 15–25 s. Trial types included no stimulus trials and trials of 40 ms bursts of 5 to 55 db above background noise pulses spaced at 5 db increments. Trials were presented across 5 blocks of 12 trials each so that no one trial was repeated in any single block. The trial types were presented in a pseudorandom order over the entire experiment. For PPI testing mice were presented with 5 trial types over 12 blocks with a variable inter trial interval of 15–25 s. Trial types included a 115 db 40 ms pulse alone trial to measure startle amplitude, and PPI trials of 20 ms bursts of a 70 or 90 db prepulse followed by the 40 ms 115 db startling pulse. For testing long ISI PPI we used prepulses presented 100 or 500 ms prior to the pulse. The trial types were presented in pseudorandom order across the experiment except for in the first and last block which contained only 6 pulse alone trials to assess initial baseline startle reactivity and habituation. Pulse alone trials from the first and middle blocks were used to calculate average startle magnitude used in PPI calculations. PPI was calculated as: [(average startle magnitude – average PPI trial startle magnitude)/(average startle magnitude)]*100. For both acoustic startle and PPI testing, startle amplitude was measured every 1 millisecond over a 100 ms period beginning at the onset of the startle stimulus. The maximum startle amplitude over this period was taken as the definitive startle magnitude if having occurred 40 ms or less following the stimulus. In mice, startle responses are measured by whole body movement and the apparent magnitude of the startle response is thus influenced by body weight (Supplementary Fig. 6A). As mutant pups were significantly smaller (Supplementary Fig. 6B), startle magnitude was normalized to body weights (g) recorded on a scale prior to testing. Locomotor activity was assessed by placing mouse pups into the corner of a novel open field chamber measuring 35×35 cm under low room lighting of ~30 lux and monitoring activity for 5 minutes using the ANY-Maze software (SDI, San Diego, CA, U.S.A.). Mice were tested during the second half of their light period. A black cloth was placed underneath four clear chambers arranged on the floor of the testing room to generate contrast, and solid white barriers were placed in between the chambers so that 4 mice could be tested at a time without seeing each other. Each chamber was divided into 9 equal square sections within the video analysis software. The inner most section was demarcated as the ‘center’ zone while the surrounding squares were marked as ‘periphery’. Distance traveled, mobility time, and speed were analyzed across the entire chamber and in

each zone. The minimum time immobile used was 5 seconds. Chambers were cleaned with 70% ethanol and dried between mice.

Histochemical techniques

The *Gsx1* probe for *in situ* hybridization in zebrafish was as previously described [42]. Antibodies used were against GFP (1:200; A-11122, Invitrogen), Kaede (1:200; PM012, MBL International), TagRFP (1:200; NC9044899, Fisher), Maguk (1:100; 73-029, NeuroMab). Image analysis was performed using ImageJ and Fluorender [43]. For *in situ* hybridization analysis in mouse, E10.5 embryos and E13.5 embryonic brains were prepared by fixation in 4% PFA in PBS followed by cryopreservation in a sucrose gradient and embedding in OCT medium as previously described [44]. Frozen sections were taken sagittally through E10.5 embryos at a thickness of 12 μm, and E13.5 brains were sectioned coronally through the brainstem at a thickness of 14 μm. Plasmids to generate *in situ* probes by *in vitro* transcription were prepared by amplification of the 3′ end (partial last exon and 3′UTR) of *Atoh1* and *Gsx1* from mouse genomic DNA and the product subsequently cloned into the pGEMT-easy vector (Promega). Primers are published in the Allen Brain Atlas (http://www.brain-map.org/). The *in situ* hybridization procedure was essentially as previously described [45]. Tissue was post fixed in 4% PFA to stop the NBT/BCIP colorimetric reaction with alkaline phosphatase (AP) and counterstained using 0.005% Nuc Fast Red (Polyscientific) then dehydrated through an EtOH gradient (50, 70, 95, 100%) and Xylene washes. Coverslips were mounted on the slides using Permount (Fisher). Photographs were taken at 5X magnification for E13.5 brains and 10X magnification for E10.5 embryos on a Zeiss Axioplan2 microscope equipped with a Leica DFC490 camera.

Statistical analysis

was performed using SPSS 17.0 (IBM, Armonk, NY) and Gnumeric 1.10.16 (http://projects.gnome.org/gnumeric/). Graphs show mean and standard error. Post-hoc tests were Bonferroni corrected for multiple comparisons as appropriate and homogenous subsets calculated using the Student-Newman-Keuls test.

Results

Transgenic line *y252* labels neurons which are required for PPI

In fish, PPI is manifest as a reduction in startle responsiveness when the prepulse precedes the intense stimulus at an ISI of 30–1000 ms, and as in mammals, suppression of the startle response is dependent on the ISI used and the prepulse intensity (Supplementary Fig. 1a)[20–21]. We used high speed video recording and computational image analysis to assess the responsiveness of zebrafish larvae to brief vibrational stimuli during startle alone and PPI trials [20]. To identify neurons required for PPI, we screened a library of transgenic zebrafish enhancer trap lines which express the Gal4 transcription factor in distinct populations of neurons (Fig. 1a). These lines were generated using a technique that restricts Gal4 expression to the nervous system, allowing functional analysis of these genetically targeted neurons in physiology and behavior [23]. Neurons labeled in each line were selectively ablated by using Gal4 to activate expression of a cytotoxin from a UAS promoter. After visually confirming ablation efficacy (Fig. 1b), larvae were tested for

changes in PPI. After ablation, PPI was reduced by 45% at an ISI of 500 ms in transgenic line *Et(REx2-SCP1:Gal4ff)y252* (*y252*) (Fig. 1c, Supplementary Fig. 1b). Unexpectedly, at ISIs of 30 and 120 ms, PPI was significantly increased (Fig. 1d) indicating that the change in PPI depended on the ISI. *y252* labels a prominent bilateral stripe of dorso-medially positioned neurons extending through the entire hindbrain continuous with the spinal cord. Transgene expression was also observed in the optic tectum, ventral forebrain and hypothalamus (Fig. 4b). After neuronal ablation in *y252*, movement kinematics during the startle response were normal indicating that changes in startle were not due to motor system defects (Supplementary Fig. 2a–d). It is unlikely that larvae failed to detect the prepulse because larvae showed an increase in startle responsiveness (Fig. 1e), and a shorter response latency (Supplementary Fig. 2e). Moreover, because groups of ablated and control larvae matched for startle responsiveness retained significant differences in PPI, these differences could not be attributed to increased startle sensitivity (Fig. 1f). The differential effect of *y252* neuron ablation on PPI at long and short ISI implies that different mechanisms mediate PPI during distinct temporal windows, consistent with findings from pharmacological and lesion studies in mammals [16]. Ablation caused additional behavioral phenotypes including a loss of responsiveness to a light flash stimulus and reduced baseline swimming activity (Fig. 1g, Supplementary Fig. 2). Despite the low baseline activity, after ablation, larvae showed a significant increase in swim distance after a change in illumination, indicative of hyperactivity (Fig. 1h). Neurons expressing Gal4 in the *y252* enhancer trap line are thus required for multiple behaviors including modulation of startle sensitivity and PPI.

Acute silencing of *y252* neurons produces startle and PPI defects

To test whether neurons in *y252* are directly required for PPI, neuronal excitability was acutely suppressed using the green light-activated proton pump Arch3 [32]. For these experiments, we established a semi-restrained preparation allowing illumination of the brain through a microscope objective, while using a stage-mounted speaker to provide an acoustic/vibrational stimulus for eliciting startle responses (Fig. 2a, b; Supplementary Fig. 3). Tail movements were monitored using a second objective, allowing us to measure startle responsiveness and PPI. We used *y252* to activate expression of a UAS:Arch3-CFP transgene and selected fish with strong CFP expression, and non-fluorescent siblings that lacked either the Gal4 (*y252*) transgene or the UAS reporter. Because acoustic startle responses are initiated with a latency of less than 20 ms after the stimulus, they were easily distinguished from locomotor responses to the sudden increments in light intensity which have broadly distributed response latencies of 100–500 ms [40]. Thus in these experiments, any tail movement observed within 20 ms of the stimulus was classified as a startle response, and illumination alone did not elicit tail movement responses during this window (paired t-test $t_{33} = 0.93$, $p = 0.36$; Fig. 2c). When illuminated *y252; UAS:Arch3* larvae showed an increase in startle responsiveness while sibling control larvae were not effected (Fig. 2b, d). We next tested PPI, using a 500 ms ISI as in our initial screen and found that illumination reduced PPI by 38% in *y252; UAS:Arch3* larvae but had no effect on siblings (Fig. 2e). Acute and reversible silencing of *y252* neurons thus phenocopied the effects of ablating these neurons confirming that transgenic line *y252* expresses Gal4 in neurons required for PPI at long ISI and regulation of the startle response threshold.

y252 neurons are primarily glutamatergic and form synapses adjacent to central neurons which initiate the startle response

To analyze how *y252* neurons are involved in PPI, we first examined their neurotransmitter profile. Prominent *y252* transgene expression was observed in a bilateral longitudinal column of dorso-medially located neurons extending along the rostro-caudal axis of the hindbrain (Fig. 3a). In the hindbrain, neurons with a defined neurotransmitter type are also arranged in distinct longitudinal columns [29, 46–47]. In transverse and dorsal sections, columns of glutamatergic, GABAergic and glycinergic neurons are seen to be intercalated with columns occupying different mediolateral positions (for example Fig. 3b) specified by a code of regionally expressed transcription factors. We characterized *y252* neurons using transgenic lines which express fluorescent proteins in glutamatergic and glycinergic columns [29, 47]. *y252* neurons were situated in the second most lateral of the four columns of glutamatergic neurons in the caudal hindbrain (Fig. b–d). Moreover, in triple transgenic *y252; UAS:nls-GFP; vGlut:DsRed* larvae, GFP and DsRed were strongly co-expressed throughout the rostro-caudal extent of the hindbrain (Fig. 3e–g), and single confocal slices confirmed that *y252* neurons were predominantly glutamatergic (Fig. 3j–l). However, scattered *y252* neurons showed co-expression with the glycinergic neuron marker, mostly in the caudal hindbrain (Fig. 3h–i and m–o).

Next we examined connections between *y252* neurons and the Mauthner cell which is localized in the brainstem and is required for short latency startle responses that are inhibited during PPI. Using *y252* to drive a membrane-tagged RFP reporter line, we found that axons from *y252* hindbrain neurons projected ventrally, running in close apposition to the lateral dendrite of the Mauthner cell and extending beneath the Mauthner cell soma and initial axon segment (Fig. 3p, q). To determine whether synaptic contacts may exist between *y252* neurons and the Mauthner cells, presynaptic terminals of *y252* neurons were marked using a synaptophysin-RFP reporter. The lateral dendrite of the Mauthner cell strongly colocalized with RFP puncta and additional sparse puncta were also observed on the soma (Fig. 3r). Immunostaining against post-synaptic density proteins confirmed that these puncta represent synapses (Fig. 3s). The post-synaptic side of glutamatergic synapses is demarcated by Maguk family proteins (PSD95/93, SAP-97) [48]. Maguk immunofluorescence opposed RFP puncta in two areas on the lateral dendrite of the Mauthner cell (Fig. 3t–w) including a region at the distal tip of the lateral dendrite, which receives acoustic input from neurons of the statoacoustic ganglion [49]. These data thus implicate glutamatergic neurons as an intrinsic part of the neuronal mechanism for PPI.

Genetic and pharmacological evidence have implicated dysregulation of glutamate signaling in schizophrenia [50–51] and glutamate receptor antagonists produce schizophrenia-like symptoms including reduced PPI [52]. After bath exposure to the NMDA receptor antagonist MK801, larvae showed increased PPI at short ISIs, reduced PPI at long ISIs and increased startle responsiveness (Fig. 3x–z) similar to the phenotype of *y252* ablated larvae and consistent with previous findings [20, 53]. These results show that *y252* neurons form synapses closely adjacent to startle initiating neurons and suggest that mechanisms involving glutamatergic neurotransmission are involved in regulating the startle response during PPI at distinct temporal windows.

y252 delineates neurons which express *Gsx1* during embryonic development

Transgenic reporters in enhancer trap lines frequently recapitulate the expression pattern of adjacent genes [54]. We used linker-mediated PCR [36] to map the integration site of the Gal4 transgene in *y252* to a locus 21 kb upstream of *genomic screen homeobox 1* (*Gsx1*) on chromosome 5 (Fig. 4a). *Gsx1* is a homeodomain containing transcription factor with a highly dynamic pattern of expression during neural development. Expression is first detected in the hindbrain and subsequently observed in several regions of the nervous system including the spinal cord, optic tectum, hypothalamus and ventral forebrain in both fish and mice (Supplementary figure 4a–e)[42, 55]. Throughout development, *Gsx1* showed a very similar neuroanatomical pattern of expression to the Gal4 reporter in *y252* (Fig. 4b, c). In the spinal cord, *Gsx1* specified neurons are reported to comprise a population of dorsally located glutamatergic interneurons as well as a late-born population of GABAergic neurons [56–57], similar to the identity of neurons in the spinal cord in *y252* (Supplementary figure 4f–h). Finally, confocal analysis of hindbrain sections of *y252* embryos stained for *gsx1* and anti-GFP demonstrated that *Gsx1* and Gal4 were co-expressed (Fig. 4d–f). Taken together, these data strongly indicate that *y252* is an enhancer trap for *Gsx1*.

Gsx1 knockout mice show impairments in PPI

Gsx1 promotes the maturation of interneurons in the mammalian subpallium, [58] and is downregulated to allow migration of interneurons into the cortical plate [59]. Cortical interneuron development is of intense interest for understanding the etiology of schizophrenia [60] and several genome-wide studies for neuropsychiatric disorders including schizophrenia have suggested the presence of vulnerability loci which map near *Gsx1* (Supplementary Table 1). To determine whether our finding that neurons with developmental expression of *Gsx1* are required for PPI in fish is relevant to neuronal mechanisms of PPI in mammals, we analyzed the expression of *Gsx1* in mouse brain regions previously reported to be linked to PPI. We first confirmed the finding that *Gsx1* is expressed in longitudinal stripes extending through the developing mouse hindbrain [55]. Using *in situ* hybridization on coronal sections through E13.5 mouse brainstem we observed robust *Gsx1* expression in discrete bilaterally symmetric domains at the ventricular zone of the neuroepithelium in the medulla (Fig. 5a–b, d). Next, we examined expression in proliferative zones which give rise to brain regions linked to PPI. Two primarily cholinergic nuclei of the mesopontine tegmentum have been implicated in PPI: the laterodorsal tegmental nucleus and the pedunculopontine tegmental nucleus (PPTg) [61–62]. Progenitors for these regions include *Atoh1* expressing cells which migrate from the rhombic lip at E10.5 [63]. *In situ* hybridization showed that *Gsx1* is expressed in a region adjacent to the *Atoh1* domain but that these transcription factors are not co-expressed (Supplementary figure 5). Two other areas that may contribute to PPI in mice are the inferior and superior colliculi [64–65]. *Gsx1* expression was observed at the ventricular zone of the neuroepithelium of both of these regions (Fig. 5c, e). We then analyzed PPI in *Gsx1* knockout mice. Because *Gsx1* homozygous knockout mice have growth retardation and a high mortality rate after post-natal day 14, it was not possible to study adult homozygous mutants [35]. Instead, we analyzed responses in mice at P20–21 which is several days after PPI is first detected [66]. When tested with a range of stimulus intensities, homozygotes showed similar weight-

normalized startle responsiveness and latency to siblings (Fig. 5f, Supplementary fig. 6a–c), indicating that knockout mice are not hearing impaired. Mutant pups showed a significant overall reduction in PPI compared to littermates (Fig. 5g, Supplementary Figure 6d). PPI in heterozygotes was not significantly different from wildtypes at this stage, nor in 8 week old juvenile mice (Supplementary fig. 6e). In posthoc tests, at a 100 ms ISI the stronger prepulse induced significantly less PPI in homozygous knockout pups than in siblings; this reduction was also significant when mutants and siblings with similar startle reactivity were compared (Fig. 5h). Thus *Gsx1* is required for normal PPI in mice suggesting that it has a conserved functional role in the development of startle modulating neurons across vertebrates. *Gsx1* likely has additional conserved functions in neuronal circuit formation because in a novel open field test, mutant mice showed reduced mobility (Fig. 5i) but during movement events, moved 45% more quickly than siblings (Fig. 5j) similar to the motility phenotype of fish after ablation of *Gsx1* neurons.

Discussion

Our findings demonstrate that neurons required for PPI show developmental expression of the homeodomain transcription factor *Gsx1*. Ablation of *Gsx1* expressing neurons produced an ISI-dependent deficit in PPI in zebrafish, and *Gsx1* knockout mice exhibited a robust reduction in PPI. Genetic manipulations offer improved cell type specificity over methods based on lesions or pharmacology for suppressing cell function. However deficits produced by ablation or gene knockout might perturb neuronal development or activate compensatory mechanisms. In our experiments this is unlikely, because optogenetic silencing of *Gsx1* expressing neurons produced a reduction in PPI indicating that these neurons are directly required for normal PPI. *Gsx1* has a dynamic pattern of expression during neuronal development, with a prominent early stripe of expression observed in the dorsal hindbrain. We found that *Gsx1* hindbrain neurons are primarily glutamatergic and form synapses in close apposition to neurons which initiate startle responses, the Mauthner cells. Together, the acute requirement for *Gsx1* neurons during PPI and the fact that they likely directly connect to central startle initiating neurons strongly argues that these neurons are an intrinsic part of the neuronal mechanism for inhibition of the startle response during PPI.

Screening zebrafish to identify components of functional neuronal circuits

To identify neurons required for PPI, we established a novel genetic screening method based on ablation of neurons in randomly generated enhancer trap lines which frequently report the expression of nearby genes. These lines can be rapidly generated, are easily mapped and provide a tool for visualizing and manipulating the targeted population of neurons [67]. Mutagenesis screens in zebrafish have been previously used to isolate gene mutations which perturb behavior [68–69]. However, it is challenging to subsequently map the underlying genetic mutation and analyze how it disrupts neural function. In invertebrates, recent studies have instead screened libraries of transgenic animals with specific patterns of reporter gene expression. The reporter is used to inactivate neurons allowing their contribution to behavior to be assessed. Like mutagenesis screens, such screens are ‘unbiased’, and therefore able to identify components of a neural pathway without *a priori* knowledge. This approach also recognizes that neurons rather than proteins are the fundamental unit of circuits [70].

Because vertebrates share a fundamental brain architecture, insights from studies in fish may help to elucidate circuits operating in the mammalian brain. PPI in fish and mammals is behaviorally similar and susceptible to disruption through similar pharmacological agents; however we recognize that differences in the underlying neuronal circuitry will likely exist. Neurons in the hindbrain are patterned according to a dorso-ventral transcriptional code similar to that which acts in the spinal cord [29, 71]. Spatially, in fish these transcription factors are expressed in distinct mediolateral domains, while in mice, progenitor domains are organized in dorsoventral stripes. The dorso-medial expression of *Gsx1* in zebrafish caudal hindbrain is therefore similar in position to expression of *Gsx1* at the dorsal ventricular zone of the medulla. Thus after finding that neurons with developmental expression of *Gsx1* are required for PPI in zebrafish, and noting the similar expression pattern of *Gsx1* during neural development in fish and mouse, we tested whether *Gsx1* is also required for PPI in mice. The PPI phenotype of *Gsx1* neuron ablated zebrafish was recapitulated in *Gsx1* knockout mice, however mice, unlike fish, did not show elevated startle sensitivity. This may reflect differences in circuits for startle control between species, but also could be due to the distinction between the effect of removing neurons from a circuit through ablation or silencing, and perturbing neuronal development through gene disruption. However, our finding that in both cases, PPI was disrupted supports the idea that *Gsx1* plays a conserved role in specifying neurons that are a key part of the neuronal circuitry for sensorimotor gating.

Circuit mechanisms for PPI

In mammals, startle responses are triggered by giant reticulospinal neurons of the pontine nucleus caudalis (PNc) which receive short latency acoustic input and make monosynaptic inputs to motor neurons in the spinal cord [19, 72]. PNc neurons show reduced electrical activity during PPI trials but the precise identity of neurons which regulate PNc neuron activity during PPI remains unclear [73–74]. Pharmacological and lesion experiments suggest that multiple neuronal mechanisms mediate PPI at different ISIs [16, 75]. PPI is intact after complete transection of structures anterior to the midbrain indicating that core circuitry for PPI resides in the brainstem [76]. Lesions in several brainstem regions disrupt PPI, including in the inferior colliculus, the superior colliculus, the substantia nigra pars reticulata, the laterodorsal tegmental nucleus (LDTg) and the pedunculopontine tegmental nucleus (PPTg) [61–62, 64–65, 77]. Intriguingly, we observed *Gsx1* expression at the ventricular zones underlying the inferior and superior colliculi, and in a region adjacent to a progenitor domain for LDTg and PPTg neurons. Tracing experiments show that PPTg neurons project to the PNc [78]. PPTg lesions reduce PPI at an ISI of between 100 and 500 ms and may also increase baseline startle amplitude [62, 75]. In recordings from rat brain slices, stimulation of the PPTg inhibits the response of giant reticulospinal neurons in the PnC to auditory input [16]. This effect can be suppressed by the application of cholinergic antagonists in the PNc, consistent with the large population of cholinergic neurons in the PPTg. Whether the PPTg directly modulates PNc reticulospinal neurons (or their presynaptic input), or acts via local interneurons in the PNc is unclear. Moreover PPTg stimulation does not inhibit PNc responses to auditory stimulation for all ISIs, and cholinergic antagonists only suppress this effect for long ISIs, indicating that the PPTg pathway and/or cholinergic signaling represents only part of the mechanism for PPI. Although most work has focused on the function of

cholinergic PPTg neurons, the PPTg contains large intermingled groups of glutamatergic and GABAergic neurons which could also regulate the PNc [79–80].

Gsx1 neurons in the zebrafish hindbrain are primarily glutamatergic. There are several mechanisms by which glutamatergic neurons could regulate Mauthner cell responsiveness. We observed strong apposition of presynaptic elements from *Gsx1* neurons with Maguk immunofluorescence on the distal part of the Mauthner cell lateral dendrite. This region receives input from the acoustic nerve leading to the possibility that *Gsx1* neurons presynaptically regulate acoustic input to the Mauthner cell [81]. Our pharmacological data suggests an important role for NMDA receptors in regulating PPI. As presynaptic NMDA receptors negatively regulate transmitter release from primary sensory neurons in rat, one possibility is that *Gsx1* neurons regulate acoustic input to the Mauthner cell through presynaptic NMDA receptors [82]. Alternatively *Gsx1* neurons may directly inhibit the Mauthner cell through metabotropic glutamate receptors. Many *Gsx1* presynaptic puncta on the Mauthner cell did not colocalize with immunostaining for Maguk, which is generally used to delineate ionotropic glutamatergic synapses [83]. These synapses may therefore represent metabotropic glutamate receptors which trigger postsynaptic inhibition of the Mauthner cell through secondary messenger cascades. In addition, it should be noted that while most hindbrain *y252* neurons were glutamatergic, a small population co-localized with a glycinergic marker. During neural development in fish, many glycinergic neurons co-express GABA [46] and *Gsx1* has an established role in specifying both glutamatergic and GABAergic neurons in the spinal cord [56–57]. Our data thus does not exclude the possibility that *y252* neurons mediate PPI through direct inhibitory signaling to the Mauthner cell.

Finally, *Gsx1* neurons may act indirectly by regulating activity in interneurons which regulate Mauthner excitability. One class of candidate neurons are the Passive Hyperpolarizing Potential neurons which regulate the Mauthner cell firing threshold [84]. Indeed electrophysiological recordings have demonstrated that PPI in fish is in part mediated by decreased excitability of the Mauthner cell. Following the prepulse, the Mauthner cell shows shunting inhibition and loss of a non-linear current response that normally drives the membrane toward its firing threshold [21–22]. However these mechanisms act on a shorter timescale than behavioral PPI indicating that additional mechanisms must be present. Because ablation produced increased startle responsiveness, increased short ISI PPI and decreased long ISI PPI, *Gsx1* neurons may regulate startle responsiveness using some or all of these mechanisms for different behavioral functions.

Neurodevelopmental defects in psychiatric disorders

Many psychiatric disorders including schizophrenia, attention deficit hyperactivity disorder, and autism spectrum disorders are believed to be caused in part by abnormalities of brain development. There is converging evidence that non-specific disruptions in developmental pathways underlie shared aspects of these diseases [1]. Several lines of evidence support the idea that schizophrenia has a strong neurodevelopmental origin, including early childhood cognitive and motor impairments and increased risk associated with pre and peri-natal events [2, 85–86]. However specific neurodevelopmental consequences remain poorly understand in part because neuroanatomical findings in schizophrenia have been

inconsistent and because progressive changes during the course of the disease make it difficult to identify developmental abnormalities [87]. Nevertheless deficits have been found repeatedly in cortical interneurons which regulate the balance of excitation-inhibition suggesting that perturbations in interneuron generation during fetal development predispose the brain to psychosis [60].

Mouse studies have revealed roles for *Gsx1* and its homolog *Gsx2* in regulating proliferation and differentiation of neuronal progenitors in ventral telencephalic regions that generate forebrain interneurons [88, 89]. Loss of *Gsx1* exacerbates defects in neurogenesis of striatal and olfactory bulb neurons seen in *Gsx2* mutants [89–90]. Gross changes in cortical interneuron populations have not been described in double *Gsx1/Gsx2* knockout mice [90], however increased *Gsx1* expression profoundly disrupts progenitor domains from which these neurons are derived and suppresses interneuron migration into the cortical plate [58–59]. In the spinal cord early expression of *Gsx1* is involved in the specification of excitatory neurons, while late expression regulates the differentiation of both excitatory and inhibitory neuronal populations [56]. Thus, perturbations in the timing of expression of *Gsx1* during neural development may lead to subtle changes in the number or molecular identity of forebrain interneurons. Genome-wide association and linkage studies for several psychiatric disorders including schizophrenia [91–92], have suggested the presence of vulnerability loci near *Gsx1* but no *Gsx1* or *Gsx2* mutations have been reported in psychiatric disorders. As knockout mice for these genes have severe postnatal defects ultimately leading to death, involvement of *Gsx1* in neurological dysfunction would most likely be due to changes in the regulation of its expression [35, 88].

PPI defects and neuronal gating dysfunction in psychiatric disorders

Gating defects are posited to represent a fundamental abnormality in schizophrenia leading to cognitive processes being overwhelmed by sensory impressions and their associations [4]. PPI is a robust measure of sensorimotor gating of the startle response and PPI deficits in schizophrenic patients correlate with the degree of thought disorder [93]. However, the neurophysiologic basis for reduced PPI in schizophrenic patients remains unclear. It has been proposed that reduced PPI in schizophrenia is due to altered activity in a modulatory circuit comprising forebrain nuclei, acting on core PPI circuits which reside in brainstem regions [94]. However PPI is impaired in unaffected relatives of schizophrenic patients, implying that PPI defects may not be secondary to psychosis but represent an independent phenotype [12, 95]. It has been suggested that PPI defects in schizophrenia reflect impaired attention to the prepulse, however some (although not all) studies have found reduced PPI in schizophrenic patients at ISIs as short at 30 ms, too brief to allow attentional modulation [96–99]. PPI defects may therefore not be a consequence of disrupted forebrain function, but rather represent an independent abnormality in brainstem circuitry for startle modulation.

An intriguing possibility is that a class of interneurons with common neurodevelopmental origins in brainstem and forebrain has a basic role gating information flow in multiple brain regions. Perturbations in these neurons would therefore produce independent disruptions in PPI and cortical information processing. Previous work has implicated *Gsx1* as a key player

in neuronal development in the telencephalon. Our study shows that neurons with developmental expression of *Gsx1* have an essential role in neuronal circuitry that is involved in PPI, thus providing a molecular link between the specification of forebrain neurons and brainstem circuits which regulate the transmission of sensory information.

Supplementary Material

Refer to Web version on PubMed Central for supplementary material.

Acknowledgments

We thank Jennifer Strykowski for zebrafish support and Victoria Carter and Daniel Abebe for mouse support. We also thank Andres Buonanno for assistance and useful discussions. This work was supported by the Intramural Research Program of the NICHD.

References

1. Rapoport JL, Giedd JN, Gogtay N. Neurodevelopmental model of schizophrenia: update 2012. Mol Psychiatry. 2012; 17(12):1228–1238. [PubMed: 22488257]
2. Jones P, Murray R, Rodgers B, Marmot M. Child developmental risk factors for adult schizophrenia in the British 1946 birth cohort. The Lancet. 1994; 344(8934):1398–1402.
3. Seidman LJ, Giuliano AJ, Meyer EC, et al. Neuropsychology of the prodrome to psychosis in the napls consortium: Relationship to family history and conversion to psychosis. Archives of General Psychiatry. 2010; 67(6):578–588. [PubMed: 20530007]
4. McGhie A, Chapman J. Disorders of attention and perception in early schizophrenia. Br J Med Psychol. 1961; 34:103–116. [PubMed: 13773940]
5. Perry W, Braff DL. Information-Processing Deficits and Thought Disorder. Am J Psychiatry. 1994; 15(1):363–367. [PubMed: 8109644]
6. Perry W, Braff DL. Information-processing deficits and thought disorder in schizophrenia. Am J Psychiatry. 1994; 151(3):363–367. [PubMed: 8109644]
7. Braff D, Stone C, Callaway E, Geyer M, Glick I, Bali L. Prestimulus effects on human startle reflex in normals and schizophrenics. Psychophysiology. 1978; 15 (4):339–343. [PubMed: 693742]
8. Hoffman HS, Ison JR. Reflex modification in the domain of startle: I. Some empirical findings and their implications for how the nervous system processes sensory input. Psychological Review. 1980; 87(2):175–189. [PubMed: 7375610]
9. Ziermans TB, Schothorst PF, Sprong M, Magnee MJ, van Engeland H, Kemner C. Reduced prepulse inhibition as an early vulnerability marker of the psychosis prodrome in adolescence. Schizophr Res. 2012; 134(1):10–15. [PubMed: 22085828]
10. Mowry BJ, Gratten J. The emerging spectrum of allelic variation in schizophrenia: current evidence and strategies for the identification and functional characterization of common and rare variants. Mol Psychiatry. 2013; 18(1):38–52. [PubMed: 22547114]
11. Quednow BB, Frommann I, Berning J, Kuhn KU, Maier W, Wagner M. Impaired sensorimotor gating of the acoustic startle response in the prodrome of schizophrenia. Biol Psychiatry. 2008; 64(9):766–773. [PubMed: 18514166]
12. Cadenhead KS, Swerdlow NR, Shafer KM, Diaz M, Braff DL. Modulation of the startle response and startle laterality in relatives of schizophrenic patients and in subjects with schizotypal personality disorder: evidence of inhibitory deficits. Am J Psychiatry. 2000; 157(10):1660–1668. [PubMed: 11007721]
13. Swerdlow N, Weber M, Qu Y, Light G, Braff D. Realistic expectations of prepulse inhibition in translational models for schizophrenia research. Psychopharmacology. 2008; 199(3):331–388. [PubMed: 18568339]
14. Fendt M, Li L, Yeomans JS. Brain stem circuits mediating prepulse inhibition of the startle reflex. Psychopharmacology (Berl). 2001; 156(2–3):216–224. [PubMed: 11549224]

15. Diederich K, Koch M. Role of the pedunculopontine tegmental nucleus in sensorimotor gating and reward-related behavior in rats. Psychopharmacology. 2005; 179(2):402–408. [PubMed: 15821954]
16. Bosch D, Schmid S. Cholinergic mechanism underlying prepulse inhibition of the startle response in rats. Neuroscience. 2008; 155(1):326–335. [PubMed: 18571866]
17. Nusbaum MP, Contreras D. Sensorimotor gating: startle submits to presynaptic inhibition. Curr Biol. 2004; 14(6):R247–249. [PubMed: 15043838]
18. Zottoli SJ, Newman BC, Rieff HI, Winters DC. Decrease in occurrence of fast startle responses after selective Mauthner cell ablation in goldfish (Carassius auratus). J Comp Physiol [A]. 1999; 184(2):207–218.
19. Koch M, Lingenhöhl K, Pilz PKD. Loss of the acoustic startle response following neurotoxic lesions of the caudal pontine reticular formation: Possible role of giant neurons. Neuroscience. 1992; 49(3):617–625. [PubMed: 1386915]
20. Burgess HA, Granato M. Sensorimotor gating in larval zebrafish. J Neurosci. 2007; 27(18):4984–4994. [PubMed: 17475807]
21. Neumeister H, Szabo TM, Preuss T. Behavioral and physiological characterization of sensorimotor gating in the goldfish startle response. J Neurophysiol. 2008; 99(3):1493–1502. [PubMed: 18199818]
22. Medan V, Preuss T. Dopaminergic-induced changes in Mauthner cell excitability disrupt prepulse inhibition in the startle circuit of goldfish. J Neurophysiol. 2011; 106(6):3195–3204. [PubMed: 21957221]
23. Bergeron SA, Hannan MC, Codore H, Fero K, Li G, Moak ZB, et al. Brain selective transgene expression in zebrafish using an NRSE derived motif. Frontiers in Neural Circuits. 2012; 6:110. [PubMed: 23293587]
24. Asakawa K, Suster ML, Mizusawa K, Nagayoshi S, Kotani T, Urasaki A, et al. Genetic dissection of neural circuits by Tol2 transposon-mediated Gal4 gene and enhancer trapping in zebrafish. Proc Natl Acad Sci USA. 2008; 105(4):1255–1260. [PubMed: 18202183]
25. Juven-Gershon T, Cheng S, Kadonaga JT. Rational design of a super core promoter that enhances gene expression. Nat Methods. 2006; 3(11):917–922. [PubMed: 17124735]
26. Davison JM, Akitake CM, Goll MG, Rhee JM, Gosse N, Baier H, et al. Transactivation from Gal4-VP16 transgenic insertions for tissue-specific cell labeling and ablation in zebrafish. Dev Biol. 2007; 304(2):811–824. [PubMed: 17335798]
27. Burgess HA, Johnson SL, Granato M. Unidirectional startle responses and disrupted left-right co-ordination of motor behaviors in robo3 mutant zebrafish. Genes Brain Behav. 2009; 8(5):500–511. [PubMed: 19496826]
28. Akitake CM, Macurak M, Halpern ME, Goll MG. Transgenerational analysis of transcriptional silencing in zebrafish. Dev Biol. 2011; 352(2):191–201. [PubMed: 21223961]
29. Kinkhabwala A, Riley M, Koyama M, Monen J, Satou C, Kimura Y, et al. A structural and functional ground plan for neurons in the hindbrain of zebrafish. Proc Natl Acad Sci U S A. 2011; 108(3):1164–1169. [PubMed: 21199947]
30. Gradinaru V, Zhang F, Ramakrishnan C, Mattis J, Prakash R, Diester I, et al. Molecular and cellular approaches for diversifying and extending optogenetics. Cell. 2010; 141(1):154–165. [PubMed: 20303157]
31. Yokogawa T, Hannan MC, Burgess HA. The dorsal raphe modulates sensory responsiveness during arousal in zebrafish. The Journal of Neuroscience. 2012; 32:15205–15215. [PubMed: 23100441]
32. Chow BY, Han X, Dobry AS, Qian X, Chuong AS, Li M, et al. High-performance genetically targetable optical neural silencing by light-driven proton pumps. Nature. 2010; 463(7277):98–102. [PubMed: 20054397]
33. Koga A, Cheah FS, Hamaguchi S, Yeo GH, Chong SS. Germline transgenesis of zebrafish using the medaka Tol1 transposon system. Dev Dyn. 2008; 237(9):2466–2474. [PubMed: 18729212]
34. Appelbaum L, Wang G, Yokogawa T, Skariah GM, Smith SJ, Mourrain P, et al. Circadian and Homeostatic Regulation of Structural Synaptic Plasticity in Hypocretin Neurons. Neuron. 2010; 68(1):87–98. [PubMed: 20920793]

35. Li H, Zeitler PS, Valerius MT, Small K, Potter SS. Gsh-1, an orphan Hox gene, is required for normal pituitary development. EMBO J. 1996; 15(4):714–724. [PubMed: 8631293]
36. Dupuy AJ, Akagi K, Largaespada DA, Copeland NG, Jenkins NA. Mammalian mutagenesis using a highly mobile somatic Sleeping Beauty transposon system. Nature. 2005; 436(7048):221–226. [PubMed: 16015321]
37. Curado S, Anderson RM, Jungblut B, Mumm J, Schroeter E, Stainier DY. Conditional targeted cell ablation in zebrafish: a new tool for regeneration studies. Dev Dyn. 2007; 236(4):1025–1035. [PubMed: 17326133]
38. Pisharath H, Rhee JM, Swanson MA, Leach SD, Parsons MJ. Targeted ablation of beta cells in the embryonic zebrafish pancreas using E. coli nitroreductase. Mechanisms of Development. 2007; 124(3):218–229. [PubMed: 17223324]
39. Issa FA, O'Brien G, Kettunen P, Sagasti A, Glanzman DL, Papazian DM. Neural circuit activity in freely behaving zebrafish (Danio rerio). J Exp Biol. 2011; 214(Pt 6):1028–1038. [PubMed: 21346131]
40. Burgess HA, Granato M. Modulation of locomotor activity in larval zebrafish during light adaptation. J Exp Biol. 2007; 210(14):2526–2539. [PubMed: 17601957]
41. Fernandes AM, Fero K, Arrenberg AB, Bergeron SA, Driever W, Burgess HA. Deep Brain Photoreceptors Control Light-Seeking Behavior in Zebrafish Larvae. Curr Biol. 201210.1016/j.cub.2012.1008.1016
42. Cheesman SE, Eisen JS. gsh1 demarcates hypothalamus and intermediate spinal cord in zebrafish. Gene Expression Patterns. 2004; 5(1):107–112. [PubMed: 15533825]
43. FluoRender: An application of 2D image space methods for 3D and 4D confocal microscopy data visualization in neurobiology research. Proceedings of the Pacific Visualization Symposium (PacificVis), 2012; Feb. 28 2012–March 2 2012; IEEE; 2012.
44. Hayes L, Zhang Z, Albert P, Zervas M, Ahn S. Timing of Sonic hedgehog and Gli1 expression segregates midbrain dopamine neurons. The Journal of Comparative Neurology. 2011; 519(15):3001–3018. [PubMed: 21713771]
45. Hayes L, Ralls S, Wang H, Ahn S. Duration of Shh signaling contributes to mDA neuron diversity. Dev Biol. 2013; 374(1):115–126. [PubMed: 23201023]
46. Higashijima S, Mandel G, Fetcho JR. Distribution of prospective glutamatergic, glycinergic, and GABAergic neurons in embryonic and larval zebrafish. J Comp Neurol. 2004; 480(1):1–18. [PubMed: 15515020]
47. Koyama M, Kinkhabwala A, Satou C, Higashijima S, Fetcho J. Mapping a sensory-motor network onto a structural and functional ground plan in the hindbrain. Proc Natl Acad Sci U S A. 2011; 108(3):1170–1175. [PubMed: 21199937]
48. Meyer MP, Trimmer JS, Gilthorpe JD, Smith SJ. Characterization of zebrafish PSD-95 gene family members. J Neurobiol. 2005; 63(2):91–105. [PubMed: 15660367]
49. Kimmel CB, Sessions SK, Kimmel RJ. Morphogenesis and synaptogenesis of the zebrafish Mauthner neuron. J Comp Neurol. 1981; 198(1):101–120. [PubMed: 7229136]
50. Moghaddam B, Javitt D. From Revolution to Evolution: The Glutamate Hypothesis of Schizophrenia and its Implication for Treatment. Neuropsychopharmacology. 2012; 37(1):4–15. [PubMed: 21956446]
51. Ayalew M, Le-Niculescu H, Levey DF, Jain N, Changala B, Patel SD, et al. Convergent functional genomics of schizophrenia: from comprehensive understanding to genetic risk prediction. Mol Psychiatry. 2012; 17(9):887–905. [PubMed: 22584867]
52. Geyer MA, Ellenbroek B. Animal behavior models of the mechanisms underlying antipsychotic atypicality. Prog Neuro-Psychopharmacol Biol Psychiatry. 2003; 27 (7):1071–1079.
53. Wolman MA, Jain RA, Liss L, Granato M. Chemical modulation of memory formation in larval zebrafish. Proc Natl Acad Sci USA. 2011; 108(37):15468–15473. [PubMed: 21876167]
54. Balciunas D, Davidson AE, Sivasubbu S, Hermanson SB, Welle Z, Ekker SC. Enhancer trapping in zebrafish using the Sleeping Beauty transposon. BMC Genomics. 2004; 5(1):62. [PubMed: 15347431]

55. Valerius MT, Li H, Stock JL, Weinstein M, Kaur S, Singh G, et al. Gsh-1: a novel murine homeobox gene expressed in the central nervous system. Dev Dyn. 1995; 203(3):337–351. [PubMed: 8589431]
56. Mizuguchi R, Kriks S, Cordes R, Gossler A, Ma Q, Goulding M. Ascl1 and Gsh1/2 control inhibitory and excitatory cell fate in spinal sensory interneurons. Nat Neurosci. 2006; 9(6):770–778. [PubMed: 16715081]
57. Satou C, Kimura Y, Hirata H, Suster ML, Kawakami K, Higashijima S. Transgenic tools to characterize neuronal properties of discrete populations of zebrafish neurons. Development. 2013; 140(18):3927–3931. [PubMed: 23946442]
58. Pei Z, Wang B, Chen G, Nagao M, Nakafuku M, Campbell K. Homeobox genes Gsx1 and Gsx2 differentially regulate telencephalic progenitor maturation. Proc Natl Acad Sci U S A. 2011; 108(4):1675–1680. [PubMed: 21205889]
59. Wang B, Long JE, Flandin P, Pla R, Waclaw RR, Campbell K, et al. Loss of Gsx1 and Gsx2 function rescues distinct phenotypes in Dlx1/2 mutants. J Comp Neurol. 2013; 521(7):1561–1584. [PubMed: 23042297]
60. Marín O. Interneuron dysfunction in psychiatric disorders. Nat Rev Neurosci. 2012; 13(2):107–120. [PubMed: 22251963]
61. Jones CK, Shannon HE. Lesions of the laterodorsal tegmental nucleus disrupt prepulse inhibition of the acoustic startle reflex. Pharmacol Biochem Behav. 2004; 78 (2):229–237. [PubMed: 15219762]
62. Prepulse inhibition of acoustic startle in rats after lesions of the pedunculopontine tegmental nucleus. 1993. [Accessed Date Accessed 1993]
63. Machold R, Fishell G. Math1 is expressed in temporally discrete pools of cerebellar rhombic-lip neural progenitors. Neuron. 2005; 48(1):17–24. [PubMed: 16202705]
64. Li L, Korngut LM, Frost BJ, Beninger RJ. Prepulse inhibition following lesions of the inferior colliculus: prepulse intensity functions. Physiol Behav. 1998; 65(1):133–139. [PubMed: 9811375]
65. Fendt M, Koch M, Schnitzler HU. Sensorimotor gating deficit after lesions of the superior colliculus. Neuroreport. 1994; 5(14):1725–1728. [PubMed: 7827317]
66. Nakamura K, Koyama Y, Takahashi K, Tsurui H, Xiu Y, Ohtsuji M, et al. Requirement of tryptophan hydroxylase during development for maturation of sensorimotor gating. J Mol Biol. 2006; 363(2):345–354. [PubMed: 16979184]
67. Scott EK, Mason L, Arrenberg AB, Ziv L, Gosse NJ, Xiao T, et al. Targeting neural circuitry in zebrafish using GAL4 enhancer trapping. Nat Methods. 2007; 4(4):323–326. [PubMed: 17369834]
68. Granato M, van Eeden FJ, Schach U, Trowe T, Brand M, Furutani-Seiki M, et al. Genes controlling and mediating locomotion behavior of the zebrafish embryo and larva. Development. 1996; 123:399–413. [PubMed: 9007258]
69. Neuhauss S, Biehlmaier O, Seeliger M, Das T, Kohler K, Harris W, et al. Genetic Disorders of Vision Revealed by a Behavioral Screen of 400 Essential Loci in Zebrafish. J Neurosci. 1999; 19(19):8603–8615. [PubMed: 10493760]
70. Pfeiffer BD, Jenett A, Hammonds AS, Ngo TT, Misra S, Murphy C, et al. Tools for neuroanatomy and neurogenetics in Drosophila. Proc Natl Acad Sci USA. 2008; 105(28):9715–9720. [PubMed: 18621688]
71. Gray PA. Transcription Factors Define the Neuroanatomical Organization of the Medullary Reticular Formation. Frontiers in Neuroanatomy. 2013:7. [PubMed: 23717265]
72. Leitner DS, Powers AS, Hoffman HS. The neural substrate of the startle response. Physiol Behav. 1980; 25(2):291–297. [PubMed: 7413836]
73. Lingenhohl K, Friauf E. Giant neurons in the rat reticular formation: a sensorimotor interface in the elementary acoustic startle circuit? J Neurosci. 1994; 14 (3 Pt 1):1176–1194. [PubMed: 8120618]
74. Carlson S, Willott JF. Caudal Pontine Reticular Formation of C57BL/6J Mice: Responses to Startle Stimuli, Inhibition by Tones, and Plasticity. J Neurophysiol. 1998; 79(5):2603–2614. [PubMed: 9582232]
75. Diederich K, Koch M. Role of the pedunculopontine tegmental nucleus in sensorimotor gating and reward-related behavior in rats. Psychopharmacology. 2005; 179(2):402–408. [PubMed: 15821954]

76. Davis M, Gendelman PM. Plasticity of the acoustic startle response in the acutely decerebrate rat. Journal of Comparative and Physiological Psychology. 1977; 91 (3):549–563. [PubMed: 874121]
77. Koch M, Fendt M, Kretschmer BD. Role of the substantia nigra pars reticulata in sensorimotor gating, measured by prepulse inhibition of startle in rats. Behav Brain Res. 2000; 117(1–2):153–162. [PubMed: 11099769]
78. Koch M, Kungel M, Herbert H. Cholinergic neurons in the pedunculopontine tegmental nucleus are involved in the mediation of prepulse inhibition of the acoustic startle response in the rat. Exp Brain Res. 1993; 97(1):71–82. [PubMed: 8131833]
79. Clements JR, Grant S. Glutamate-like immunoreactivity in neurons of the laterodorsal tegmental and pedunculopontine nuclei in the rat. Neurosci Lett. 1990; 120(1):70–73. [PubMed: 2293096]
80. Wang H-L, Morales M. Pedunculopontine and laterodorsal tegmental nuclei contain distinct populations of cholinergic, glutamatergic and GABAergic neurons in the rat. Eur J Neurosci. 2009; 29(2):340–358. [PubMed: 19200238]
81. Eaton R, Farley R, Kimmel C, Schabtach E. Functional development in the Mauthner cell system of embryos and larvae of the zebra fish. J Neurobiol. 1977; 8(2):151–172. [PubMed: 856948]
82. Bardoni R, Torsney C, Tong CK, Prandini M, MacDermott AB. Presynaptic NMDA receptors modulate glutamate release from primary sensory neurons in rat spinal cord dorsal horn. J Neurosci. 2004; 24(11):2774–2781. [PubMed: 15028770]
83. Gardoni F, Marcello E, Di Luca M. Postsynaptic density-membrane associated guanylate kinase proteins (PSD-MAGUKs) and their role in CNS disorders. Neuroscience. 2009; 158(1):324–333. [PubMed: 18773944]
84. Weiss SA, Preuss T, Faber DS. A role of electrical inhibition in sensorimotor integration. Proc Natl Acad Sci U S A. 2008; 105(46):18047–18052. [PubMed: 19004764]
85. Brown AS. Epidemiologic studies of exposure to prenatal infection and risk of schizophrenia and autism. Devel Neurobio. 2012; 72(10):1272–1276.
86. Clarke MC, Harley M, Cannon M. The Role of Obstetric Events in Schizophrenia. Schizophrenia Bulletin. 2006; 32(1):3–8. [PubMed: 16306181]
87. Lewis DA, Levitt P. SCHIZOPHRENIA AS A DISORDER OF NEURODEVELOPMENT. Annu Rev Neurosci. 2002; 25(1):409–432. [PubMed: 12052915]
88. Szucsik JC, Witte DP, Li H, Pixley SK, Small KM, Potter SS. Altered forebrain and hindbrain development in mice mutant for the Gsh-2 homeobox gene. Dev Biol. 1997; 191(2):230–242. [PubMed: 9398437]
89. Toresson H, Campbell K. A role for Gsh1 in the developing striatum and olfactory bulb of Gsh2 mutant mice. Development. 2001; 128(23):4769–4780. [PubMed: 11731457]
90. Yun K, Garel S, Fischman S, Rubenstein JL. Patterning of the lateral ganglionic eminence by the Gsh1 and Gsh2 homeobox genes regulates striatal and olfactory bulb histogenesis and the growth of axons through the basal ganglia. J Comp Neurol. 2003; 461(2):151–165. [PubMed: 12724834]
91. Sullivan PF, Lin D, Tzeng JY, van den Oord E, Perkins D, Stroup TS, et al. Genomewide association for schizophrenia in the CATIE study: results of stage 1. Mol Psychiatry. 2008; 13(6): 570–584. [PubMed: 18347602]
92. Hong KS, Won H-H, Cho E-Y, Jeun HO, Cho S-S, Lee Y-S, et al. Genome-widely significant evidence of linkage of schizophrenia to chromosomes 2p24. 3 and 6q27 in an SNP-Based analysis of Korean families. American Journal of Medical Genetics Part B: Neuropsychiatric Genetics. 2009; 150B(5):647–652.
93. Perry W, Geyer MA, Braff DL. Sensorimotor gating and thought disturbance measured in close temporal proximity in schizophrenic patients. Arch Gen Psychiatry. 1999; 56(3):277–281. [PubMed: 10078506]
94. Kumari V, Gray JA, Geyer MA, ffytche D, Soni W, Mitterschiffthaler MT, et al. Neural correlates of tactile prepulse inhibition: a functional MRI study in normal and schizophrenic subjects. Psychiatry Research: Neuroimaging. 2003; 122(2):99–113. [PubMed: 12714174]
95. Kumari V, Das M, Zachariah E, Ettinger U, Sharma T. Reduced prepulse inhibition in unaffected siblings of schizophrenia patients. Psychophysiology. 2005; 42(5):588–594. [PubMed: 16176381]

96. Dawson ME, Schell AM, Hazlett EA, Nuechterlein KH, Filion DL. On the clinical and cognitive meaning of impaired sensorimotor gating in schizophrenia. Psychiatry Research. 2000; 96(3):187–197. [PubMed: 11084215]

97. Braff DL, Grillon C, Geyer MA. Gating and habituation of the startle reflex in schizophrenic patients. Arch Gen Psychiatry. 1992; 49(3):206–215. [PubMed: 1567275]

98. Kumari V, Soni W, Sharma T. Normalization of information processing deficits in schizophrenia with clozapine. Am J Psychiatry. 1999; 156(7):1046–1051. [PubMed: 10401450]

99. Hong LE, Summerfelt A, Wonodi I, Adami H, Buchanan RW, Thaker GK. Independent domains of inhibitory gating in schizophrenia and the effect of stimulus interval. Am J Psychiatry. 2007; 164(1):61–65. [PubMed: 17202545]

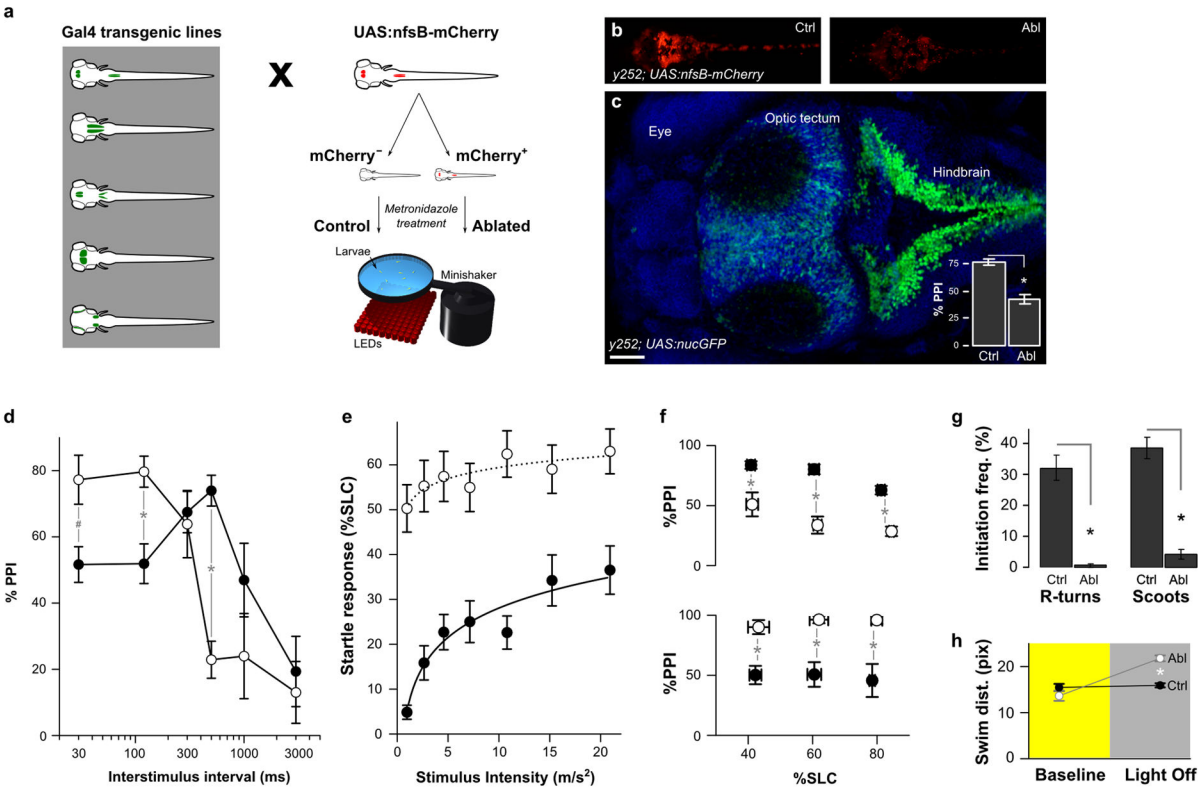

Figure 1. Neurons that modulate startle sensitivity and prepulse inhibition are identified by enhancer trap line y252

(a) Schematic of the screen used to identify neurons required for PPI. Gal4 enhancer trap lines were crossed to a *UAS:nfsB-mCherry* transgenic line and sorted into mCherry expressing and non-expressing groups. Both groups were treated from 3–5 dpf with metronidazole for ablation of nitroreductase-mCherry expressing neurons. Behavioral testing was performed after 24 h recovery from the treatment. For screening, a 500 ms ISI was used.

(b) *y252; UAS:nfsB-mCherry* larvae maintained in embryo medium (ctrl) or in medium supplemented by 10 mM metronidazole for 48 h (ablated).

(c) Dorsal confocal projection of *y252; UAS:nls-GFP* larva showing the distribution of neurons expressing the Gal4 transgene (green), counterstained with DAPI (blue). Inset shows the mean and standard error of %PPI values for *y252* control (N=47) and ablated (N=48) larvae. * $P < 0.001$. Scale bar 50 μm.

(d) Changes in PPI at different ISIs after neuronal ablation in *y252; UAS:nfsB-mCherry* larvae (open circles) compared to sibling controls (filled). N= 15–32 larvae per group. ANOVA significant interaction between ablation status and interstimulus interval $F_{5,257} = 10.23$, $p < 0.001$. # $p < 0.05$. * $p < 0.01$.

(e) Startle responsiveness (percentage of fish initiating a short latency c-start response, %SLC) in *y252* ablated larvae (open circles, N = 41) compared to sibling controls (filled, N = 27). Main effect of ablation $F_{1,66} = 26.58$, $p < 0.001$. Comparisons between ablated and controls at all stimulus intensities are significant, $p < 0.001$.

(f) PPI at 500 ms ISI (top) and 30 ms ISI (bottom) in subsets of *y252* ablated larvae (open circles) and sibling controls (filled) with similar startle responsiveness. Larvae were binned according to startle responsiveness (%SLC) in three groups: 30–50, 51–70 and 71–90. N=16–47 larvae per group. t-test * $p < 0.01$.
(g) Reduced locomotor activity after *y252* ablation. Larvae initiate two types of swimming movements, routine turns (R-turns) and slow swims (scoots) both of which are significantly reduced. N = 5 groups controls, 3 groups ablated larvae. * $p < 0.001$.
(h) Distance travelled (pixels) per swim bout in *y252* ablated larvae (Abl, grey) and controls (Ctrl, black) during baseline activity (yellow background) and movement in response to sustained darkness (grey background). N=36 larvae each group. * $p < 0.001$.

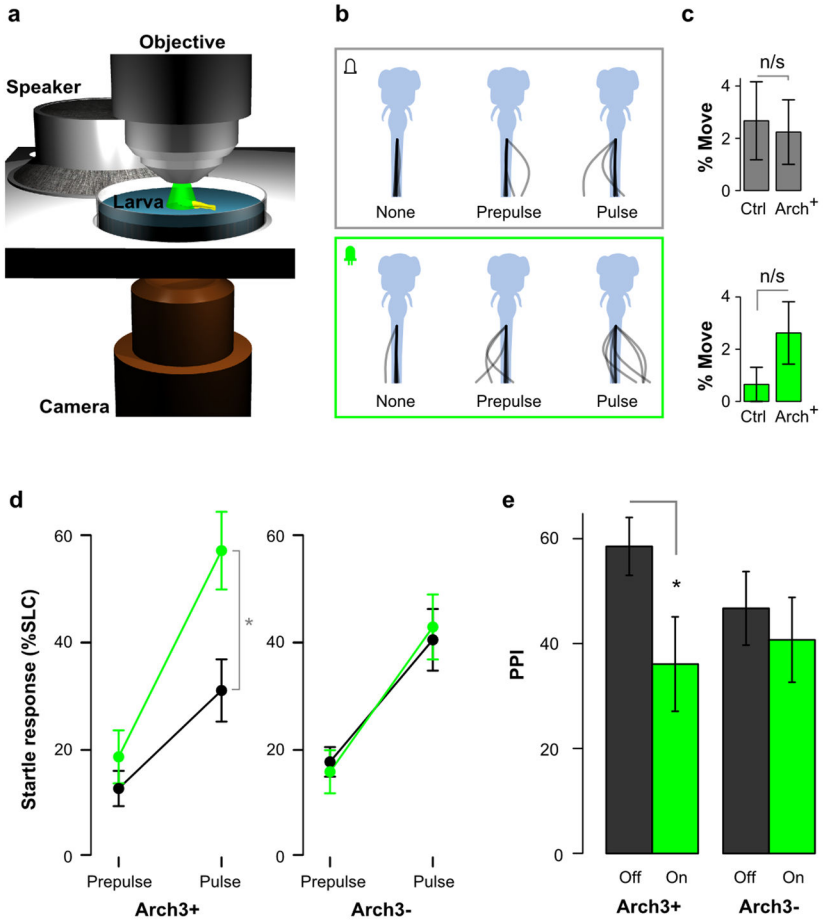

Figure 2. Acute suppression of activity in *y252* neurons reduces PPI

(a) Apparatus for Arch3 experiments using semi-restrained larvae tested on a microscope stage fitted with a speaker.

(b) Representative example of tail movement responses for an Arch3 expressing larva under baseline conditions (top) and during LED illumination (bottom), during no stimulus trials, prepulse only trials and pulse only trials.

(c) Frequency of tail movement initiation within a 15 ms window during baseline conditions without a stimulus (top) and during LED illumination (bottom). No significant differences were found between Arch3 expressing larvae and controls (N=18, 17 respectively).

(d) Startle responsiveness in Arch3 expressing *y252* larvae (N=18, Arch3+) and non-expressing siblings (N=17, Arch3−) when tested while illuminated with intense green light (green) or when not illuminated (black). Repeated measures ANOVA, interaction of light and Arch3 expression, $F_{1,33} = 12.06$, $p = 0.001$. paired t-test * $p < 0.001$.

(e) PPI during green light illumination (on) or in the dark (off) in Arch3 expressing *y252* larvae ($Arch3^{+}$, N=13, paired t-test $t_{12} = 2.66$, * p=0.021) and siblings not expressing the Arch3 transgene ($Arch3^{-}$ N=14, $t_{13} = 1.24$, p=0.24).

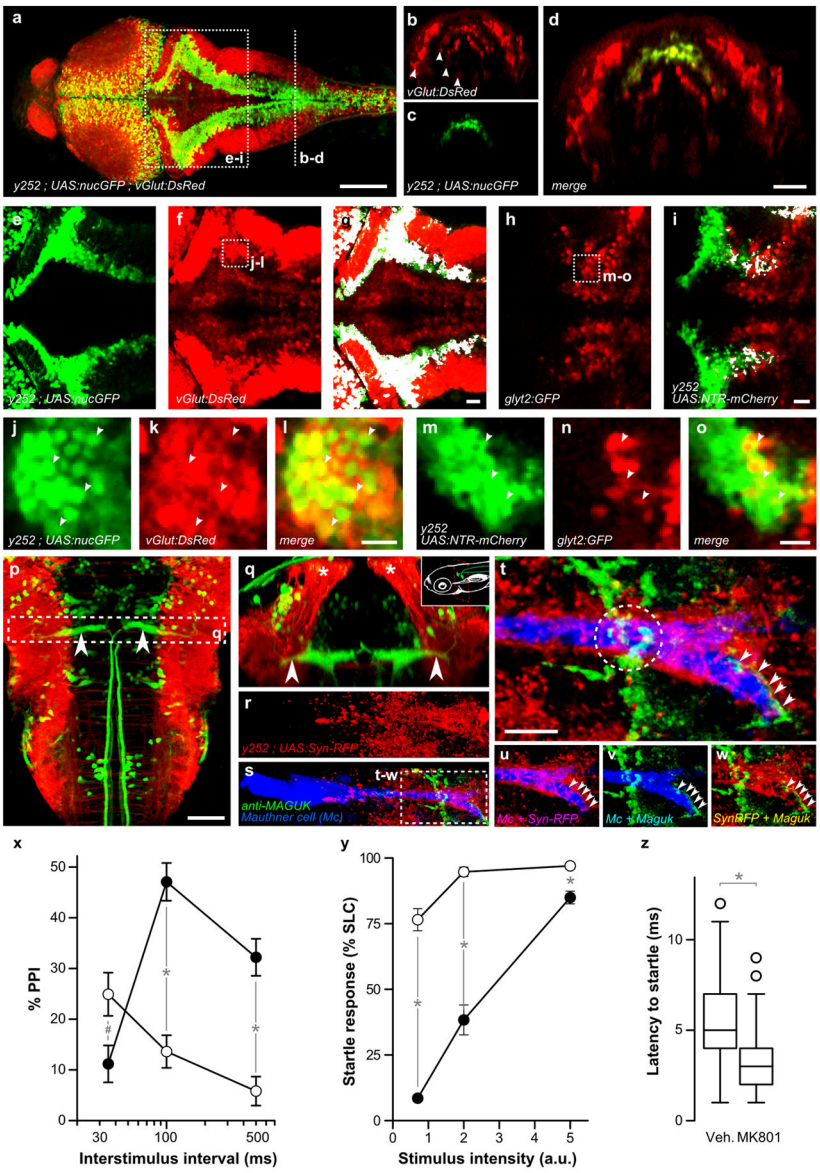

Figure 3. Hindbrain neurons in *y252* form glutamatergic synapses adjacent to the Mauthner cell

(a) Projection of a dorsal confocal stack in *y252; UAS:nlsGFP; vGlut:DsRed* larva showing *y252* expression (green) and glutamatergic neurons (red). Scale bar 100 μm.

(b–d) Coronal view of the caudal hindbrain, representing a 4 μm section derived from rotation of a dorsal confocal stack at the rostro-caudal level indicated in (a) showing that *y252* GFP+ nuclei (c, green) are located in the second-most lateral of four mediolateral stripes of glutamatergic neurons (b, red, arrowheads). Scale bar 50 μm.

(e–i) Projection of dorsal confocal sections in the region indicated in (a) showing colocalization (g,i white) between *y252* neurons (e, green) and glutamatergic neurons (f, red; *vGlut:DsRed*) or glycinergic neurons (h, red; *glyt2:GFP*, note that GFP is pseudocolored red). For (i) we used *y252; UAS:nfsB-mCherry* and pseudocolored the *y252* pattern in green after imaging for comparison with (e–g). Scale bar 20 μm.

(j–o) Single confocal sections of the regions indicated in (f) and (h) showing colocalization between *y252; UAS:nlsGFP* (j, green) and *vGlut:dsRed* (k, red), and *y252; UAS:nfsB-mCherry* (m, pseudocolored green) and *glyt2:GFP* (n, pseudocolored red). Scale bar 10 μm.
(p) Dorsal confocal projection in *y252; UAS:lynTagRFPT; J1229* larva showing the Mauthner cell (green, arrowheads) and midline projections of *y252* axons (red). J1229 is an enhancer trap line that expresses GFP in the Mauthner cell and other reticulospinal neurons [27]. Scale bar 50 μm.
(q) Coronal projection at the region indicated in (p) showing ventral projections from dorsally positioned *y252* neurons (red, asterisk) passing beside the lateral dendrite of the Mauthner cell (arrowheads). Inset schematic shows plane of section.
(r–w) *y252; UAS:Synaptophysin-RFP; J1229* larva stained with anti-Maguk revealing presynaptic puncta formed by *y252* neurons (red), the Mauthner cell (blue) and glutamatergic postsynaptic densities (green).
(t) Closer view of the lateral dendrite outlined in (s). Arrows and dotted circle mark two distinct regions where synapses from *y252* neurons are closely opposed to glutamatergic postsynaptic densities. Scale bar 10 μm.
(u–w) Split channels from (t). Colocalization between *y252* presynaptic puncta and the Mauthner cell (u, magenta), MAGUK and the Mauthner cell (v, teal) and presynaptic *y252* puncta and postsynaptic MAGUK proteins (w, yellow).
(x) PPI in larvae treated with MK-801 (open circles) or vehicle (closed circles). N=15 groups each (20 larvae per group). Main effect of treatment $F_{1,28} = 15.8$, $p < 0.001$; Interaction of treatment and ISI $F_{2,56} = 40.4$, $p < 0.001$. # $p = 0.021$, * $p < 0.001$.
(y) Startle responsiveness in larvae treated with MK-801 (open circles) or vehicle (closed circles). N=6 groups of 25 fish each. Main effect of treatment $F_{1,10} = 180.35$, $p < 0.001$. * $p < 0.01$.
(z) Reaction time (startle latency). N=334 and 343 responses for MK801 and vehicle treated larvae. * $p < 0.001$.

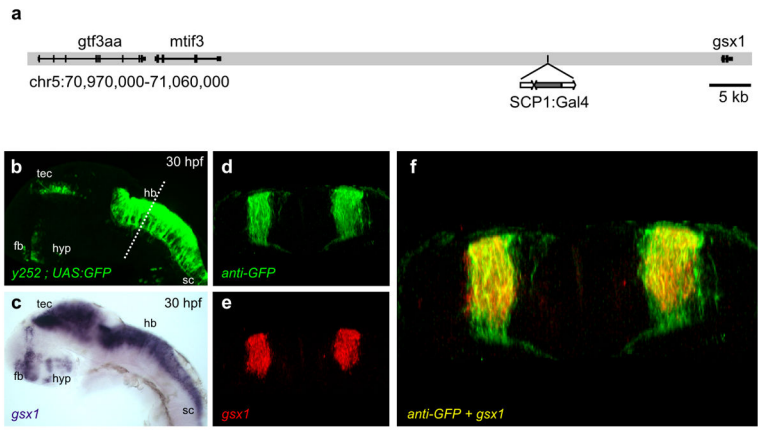

Figure 4. *y252* is an enhancer trap for Gsx1

(a) Schematic of the *y252* transgene integration site on chromosome 5. Genome edition Zv9.

(b) Lateral epifluorescent image of *y252; UAS:GFP* embryo at 30 hpf. Forebrain (fb), optic tectum (tec), hypothalamus (hyp), hindbrain (hb), spinal cord (sc).

(c) Lateral image of *in situ* hybridization for *Gsx1* at 30 hpf.

(d–f) Coronal section through the hindbrain in *y252; UAS:GFP* embryos showing GFP (d), fluorescent *in situ* hybridization signal for *Gsx1* (e) and single confocal slice merge (f).

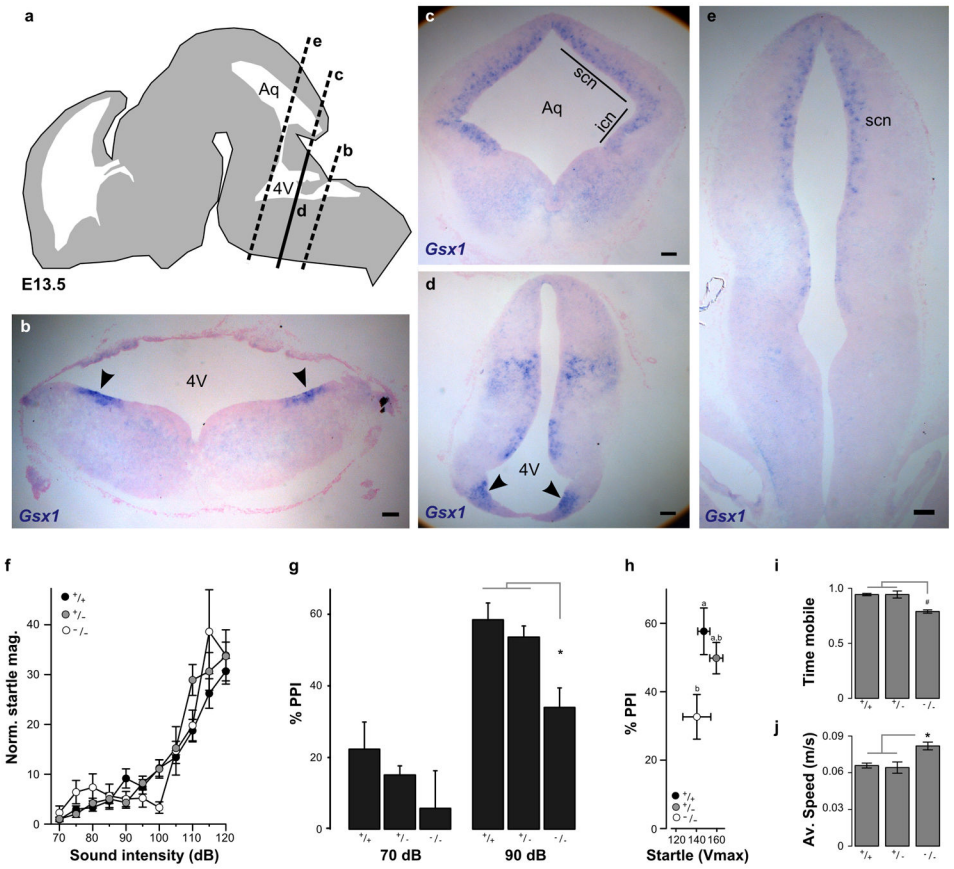

Figure 5. *Gsx1* is required for PPI in mammals

(a) Schematic of E13.5 mouse embryonic brain showing coronal planes of section through the brainstem for RNA *in situ* hybridization with *Gsx1* probe in (b–e).

(b) Dorso-lateral expression domains of *Gsx1* at the ventricular zone of the neuroepithelium in caudal hindbrain (arrowheads).

(c) Coronal section at the level of the aqueduct (Aq) showing expression of *Gsx1* in ventricular zone of the superior colliculus (scn) and inferior colliculus (icn).

(d) Same plane of section as in (c) through the 4th ventricle (4V) showing *Gsx1* expression at the ventricular zone of the pons (arrowheads).

(e) Rostral brainstem section showing *Gsx1* expression in the ventricular neuroepithelium of the superior colliculus (scn). Scale bars (b–e) 100 μm.

(f) Startle magnitude in *Gsx1* knockout mice and littermates, normalized by body weight (Vmax/g). Knockouts (open circles, N=10) show similar startle sensitivity to wildtype (black, N=15) and heterozygotes (grey, N=14).

(g) PPI in *Gsx1* knockout mice (N=13) compared to wildtype (N=17) and heterozygous siblings (N=33) at a 100 ms ISI at the indicated prepulse intensities. Repeated measures ANOVA $F_{1,61} = 4.99$, $p = 0.029$. Genotypes are indicated. * $p < 0.01$.

(h) PPI in subgroups of mice from (g) with similar startle magnitudes (not adjusted for body weight), using mice with a mean response magnitude of between 100 and 200 (Vmax). ANOVA for genotype $F_{1,28} = 6.49$, $p = 0.017$. Posthoc homogeneous subsets are indicated.

(i–j) Locomotor activity in novel open field. Fraction of time (5 minute trials) spent mobile (i) and average speed during mobile periods (j) for wildtype (N=23), heterozygous (N=31) and homozygous *Gsx1* knockout mice (N=16). # $p < 0.05$. * $p < 0.01$.